


Spring 2017

# Assessment of Short-Term Toxicity of Titanium Dioxide Nano Fiber (TDNF) in Sprague Dawley Rats

Daniel Hunter

# ASSESSMENT OF SHORT-TERM TOXICITY OF TITANIUM DIOXIDE NANO FIBER (TDNF) IN SPRAGUE DAWLEY RATS

by

DANIEL HUNTER

(Under the Direction of Worlanyo Gato)

## ABSTRACT

Nanotechnology is easily becoming one of the fastest growing markets around the globe. Synthetic nanomaterials have many unique chemical and physical properties, mainly due to their huge specific surface area and chemical makeup. Specifically, titanium dioxide ($TiO_2$) nanomaterials have high stability, anticorrosive and photocatalytic properties. These nanomaterials have applications for semiconductor photocatalysis, treatment of water, as a photoactive material in nanocrystalline solar cells, and medicine. However, not much is known about the toxicity of $TiO_2$ in the nanofiber form. The objective of the present study is to investigate the adverse effects associated with acute ingestion of $TiO_2$ nanofiber (TDNF). TDNF was fabricated via an electrospinning method, followed by dispersion in water. Six to seven week old male Sprague Dawley rats were exposed to a total of 0, 40 and 60 ppm of TDNF for two weeks via oral gavage. Weight gain and cumulative weight eaten was tracked during the course of the study, displaying statistically insignificant concentration-dependent alterations among the three treatment groups. Differences in organ weights were not statistically significant among treatment groups. Blood serum was tested for Albumin, Alanine aminotransferase, and Lactase dehydrogenase to detect tissue damage in the lungs, liver, and kidney. Results from the

blood serum indicated possible damage with respect to the kidney and liver. These findings were followed by global gene expression analysis to identify which transcripts might be responsive to TNDF toxicity. Differentially expressed mRNA levels among the liver, kidney, and lung yielded interesting results. Further analysis is needed to interpret what is being done to the tissue. One theory is the fact that TNDF is unable to penetrate the cell as a result; it forms a phagocytosis site and thus triggers inflammatory and immune response. All results taken together, short-term ingestion of titanium dioxide nano fiber (TNDF) produced marginal effects indicative of toxicity.

KEYWORDS: Nanomaterials, Titanium dioxide, Gene expression, Blood serum, Toxicity

# ASSESSMENT OF SHORT-TERM TOXICITY OF TITANIUM DIOXIDE NANO FIBER (TDNF) IN SPRAGUE DAWLEY RATS

by

DANIEL HUNTER

B. S., Georgia Southern University, 2014

A Dissertation Submitted to the Graduate Facility of Georgia Southern University in Partial Fulfillment of the Requirements for the Degree

MASTER OF SCIENCE

STATESBORO, GEORGIA

# ASSESSMENT OF SHORT-TERM TOXICITY OF TITANIUM DIOXIDE NANO FIBER (TDNF) IN SPRAGUE DAWLEY RATS

by

DANIEL HUNTER

Major Professor: Worlanyo Gato
Committee: Amanda Stewart
Ji wu

Electronic Version Approved:

May 2017

TABLE OF CONTENTS

Page

# List of Tables

**TABLE**

## List of Figures

**FIGURES**

# Chapter 1: Background/Introduction

The past decade has seen an explosive growth in the synthesis and use of engineered nanomaterials (ENMs).[1] ENMs have applications in various kinds of materials and processes because of their unique electrical, magnetic, optical, and catalytic properties.[2] Titanium dioxide nanoparticles (TDNP) are one of the most produced ENMs in the past. This is largely due to the unique characteristics that TDNP exhibit, including photocatalysis, high refractive indices, excellent anticorrosive properties, etc.[3] These characteristics allowed TDNP's to be applied in all fields of science such as electronics, transportation, telecommunication, imaging, biomedical, pollution, medication, cosmetics, coatings, etc.[4] This has led to a growth of studies that examined the toxicity of titanium dioxide in its nanoparticle form.[5] Previous research has shown that $TiO_2$ can be dangerous in *in vitro* models. For instance, a study a few years ago found that exposure of BEAS-2B cells to $TiO_2$ nanoparticles induced apoptosis and oxidative stress.[6] Another study investigated the effect of $TiO_2$ NPs on human astrocyte and neuronal cells after acute and long-term exposure.[7] Both acute and prolonged exposures, even at low dose, seem to affect the proliferative capacity of the cells. The authors found toxicological effects on the central nervous system (CNS). However, there are very little studies that have examined ENMs in their fiber form, such as the titanium dioxide nano fiber (TDNF).

TDNFs share the same chemical properties as TDNPs except for shape and can be found in common household products such as cosmetics, certain food, rubber, etc.[4c] Since these products are used frequently, contact is inevitable. Interestingly enough, the shape of the ENM plays a crucial role in nanotoxicity, as nanofibers, in theory, have a greater resistance to be broken down by an organism's internal resistance. For example, macrophages can envelope nanoparticles and essentially digest them; however, the length of the nanofibers are long enough to prevent a macrophage from breaking them down and even has a chance to lyse open the

macrophage.[8] Thus, it is essential that the toxic impact of TDNF on human health be studied thoroughly. Recent studies have shown that ENM's can have great potential to be toxic when introduced to the environment.[9] Another study has shown that a buildup of TDNF in the body can cause all sorts of problems like increased generation of reactive oxygen species (ROS) and inflammation and increased lipid peroxidation.[8, 10] One can assume that the toxicity of nanoparticles varies depending on type of ENM, exposure route and size of the material, which causes inconsistent results in ENM toxicity.[3b] The goal of the present study is to investigate the short-term effects of titanium dioxide nanofibers on the kidneys, liver, and lungs of male Sprague Dawley rats.

All organs are vital in the human body and the kidney is no exception. The kidneys are responsible for filtering out the blood by removing wastes. The kidney controls the body's fluid balance and also regulates the balance of electrolytes.[11] As nanoparticles enter the body they are small enough to enter the bloodstream, which makes contact with the kidneys a sure thing.[12] One study indicates that when Wistar rats were given palladium nanoparticle doses, the kidneys had suffered severe renal tubular dysfunction. ENM induced toxicity to the kidney can be very dangerous and very hard to detect, requiring multiple analytical techniques.[13]

The liver, like the kidney, is responsible for filtering out the blood; however, unlike the kidney the blood is filtered from the digestive track before passing on to the rest of the body. Hepatic function also includes detoxing chemicals and metabolizing drugs, making them the object of focus in toxicological examinations.

The lungs are a vital part of life for land animals, as they provide the body with oxygen by storing it via the alveoli in our lungs. Lungs are observed when doing toxicological studies with macro-drugs, even more so, with ENMs being prime candidates for drug delivery systems.

Since translocation of drugs is a vital part of toxicological studies, especially with ENMs since their high surface area to size ratio, it is important to see if it is possible for TDNF to access areas of the body not associated with the digestive tract.

This study aims for a better understanding on the renal, hepatic, and lung deficiencies of oral ingestion of TDNF in Sprague Dawley rats, using a variety of analytical tools and techniques. Gene expression analysis of transcripts involved in inflammation, apoptosis, cell growth regulation, stressors and immune response were undertaken. Furthermore, rat morphometric indices, scanning electron micrograph (SEM) and histopathology of renal tissues were performed to further characterize tissue damage via TDNF ingestion.

# Chapter 2: Materials and Methods

## 2.1 Synthesis and Characterization

The fabrication of titanium dioxide nanofibers ($TiO_2$ NF) began with mixing ~1 gram of polyvinylpyrrolidone (PVP) with 10 mL of ethanol. In a separate container ~3 grams of TiIP (titanium iso-propoxide) was mixed with 5 mL of ethanol and 3 mL of Acetic Acid. These solutions were vortexed separately for ~ 30 minutes to ensure thorough mixing. The solutions were then added together and vortexed again for another 5 minutes. This mixture was then sonicated for 20 minutes before electrospinning. Once the gelation of the intended nanofiber solution was completed, it was ready for electrospinning. The parameters of electrospinning were as follows: the distance from the end of the syringe to the grounding aluminum collector was 12-15 cm. The pumping rate of sol-gel solution was 5 mL/hr. The applied DC voltage was 25 kV. Once all the sol-gel solution had been electrospun, fabricated fibers were left overnight for complete gelation. These nanofibers were annealed at ~565°C in air for roughly 12 hours. A Field Emission Electron Microscopy (JEOL JSM-7600F) attached with Transmission Electron Detector (TED) was utilized for morphology and structural characterization. Once the inorganic $TiO_2$ nanofibers were fabricated and purified, scanning electron microscopy (SEM) and Brunaur-Emmett-Teller instruments was used to characterize the fibers.

## 2.2 Experimental Design

Twelve male Sprague Dawley rats were purchased from Taconic Bioscience Inc., Hudson NY. The rats randomly selected into three treatment groups: control (0ppm), Low (40ppm), Medium (60ppm). The rats (6-7 weeks old) were given treatment specific doses of titanium, via oral gavage, two times a week for two weeks. During the treatment period the weights of the

animals and dietary statistics were taken. At the end of the treatment period the rats were euthanized and blood was collected via cardiac puncture. Most of the kidney, liver, and lungs were extracted and preserved with liquid nitrogen, while a small fraction was submerged in a 10% formalin solution for histology and haemotoxylin and eosin (H&E) staining.

Animals were housed at the Georgia Southern University Animal Facility (1176A Biological Sciences Fieldhouse). This facility is accredited by Association for Assessment and Accreditation of Laboratory Animal Care (AAALAC). Rats were treated according to the principles outlined in the ILAR's (Institute for Laboratory Animal Research) Guide for Care and Use of Laboratory Animals. Protocols were reviewed and approved by Institutional Animal Care and Use Committee (IACUC protocol# I15002). Care was taken to minimize the number of animals employed in the research as well as minimizing animal discomfort.

## 2.3 Why In Vivo?

The *In vivo* testing method was used as it accurately simulates an organism's biological environment; however, it should be noted that it is rather difficult to extrapolate data from a rodent and apply it to humans.

## 2.4 Microarray Experiment

Total RNA was converted to single-stranded sense-target, fragmented, labeled, and hybridized to the Affymetrix Rat Gene ST 2.0 microarray according to the manufacturer's protocol (Affymetrix, Catalog no. 902280). The labeling kit is the GeneChip® WT PLUS Reagent Kit (Affymetrix, catalog no. 902414). After hybridization, arrays were washed on the Affymetrix 450S Fluidics unit and scanned using the Affymetrix 7G scanner as described in Affymetrix

GeneChip™ Wash, Stain and Scan protocol (Affymetrix, 2008). The Rat Gene ST 2.0 chip contains over 27,000 protein-coding transcripts and over 24,000 Entrez genes. Microarray was used to determine gene expression levels of select genes transcripts.

2.5 Quantitative PCR

Quantitative PCR was used to determine changes in genotypic expression. Quantitative measurement of Igha, CD209, Hepacam2, Rgs13, IgG2a, TNF-α, IL-1β, NF-kB, p53, p21, Gadd45α and β-actin as control gene. These transcripts play such cellular roles as immune response, DNA transcription and recombination, regulating cell division, negatively regulating G-protein signal pathways, and cell structure and motility. Quantification of the transcripts was measured using quantitative real-time polymerase chain reaction (RT-qPCR) using β-actin as a control gene. FASTA mRNA sequences of these mRNA transcripts were obtained for *Rattus Norvegicus* using the National Center for the Biotechnology Information (NCBI) database. Forward and reverse primers for the genes were then generated using NCBI Primer-Blast. Primer sequences were shown in Table 1. Primers were purchased from Integrated DNA Technologies Inc (IDT), Coralville IA USA.

Total RNA was extracted from rat livers using a Qiagen miRNEAsy mini kit (Qiagen, Catalog no. 217004). Approximately 30 mg kidney samples were homogenized in Qiazol buffer. Qiazol buffer denatures and inactivates RNases, separating RNA into the aqueous phase and DNA and proteins into the organic phase. The aqueous phase with RNA is then allowed to bind to a silica-gel membrane, DNAse treated, washed, and finally eluted with RNase-free water. Total RNA was quantified using the UV-vis spectrophotometer at 260 and

280 nm absorbance. RNA integrity was evaluated on the Agilent 2100 Bioanalyzer 6000 Nano assay (Agilent, catalog no. 5067-1511).

## 2.6 Clinical Serum

### 2.6.1 Total Protein

In this experiment, serum total protein was quantified using Randox Monza Chemistry analyzer instrument (Kearneysville WV). The assay was performed according to the Randox's total protein biuret assay guidelines. Briefly, standards and samples were prepared according to the manufacturer's protocol and quantified on the instrument at a wavelength of 546 nm.

### 2.6.2 Albumin

The Shimadzu UV-VIS Recording Spectrophotometer was used to quantify the amount of albumin (ALB) in the blood serum. Method of ALB determination was used with the bromocresol green (BCG) method; 10 µl of sample was mixed with 1ml of BCG. Absorbance was taken within 90 seconds of mixing at 630 nm at a constant temperature of 37 $^{o}$C. Concentration of ALB was calculated using linear extrapolation via ALB standard curve; using the BCG reagent as a blank and a 6g/dL ALB solution as the upper limit.

### 2.6.3 Alanine Aminotransferase

The RX Monza was used to quantify the amount of alanine aminotransferase (ALT) in the blood. RX Monza was calibrated with a Calibration Serum Level 3 (CAL 3) from Randox Laboratory. The CAL 3 serum had to be primed before use; therefore, 5ml of DI water was added to the CAL 3 powdered mix and was left in darkness for 30 mins. ALT kit from Randox was used to

determine ALT levels. ALT reagent was prepared by mixing 2 ml of R1a with R1b, from the ALT kit. The upper calibration limit was prepared using 50 µl of CAL 3 solution with 500ul of R1a/b solution (1:10 sample to reagent ratio). The blank used was just the R1a/b mixture by itself. RX Monza used linear calibration to determine ALT levels in sample.

2.6.4 Lactase Dehydrogenase

The Rx Monza analyzer (Randox Laboratories, Kearneysville WV) was employed to quantitatively determine the amount of lactase dehygrogenase (LDH) in the blood serum. LDH test was optimized using LDH Pyruvate-L-lactated kit from Randox laboratories (Kearneysville WV). Rx Monza instrument was calibrated using the CAL 3 serum (Cat#: CAL2351). Once calibrated, the LDH reagent was prepared by mixing one vial of R1b with 3ml of R1a from the LDH Randox kit. Samples were prepared and measured according to guidelines provided Randox laboratories (Kearneysville WV).

2.6.5 Igha Levels in Liver

Quantification of Igha was measured using quantitative real-time polymerase chain reaction (qRT-PCR) using β-actin as a control gene. FASTA mRNA sequences of these mRNA transcripts were obtained for Rattus norvegicus using the National Center for the Biotechnology Information (NCBI) database. Forward and reverse primers for the genes were then generated using NCBI Primer-Blast. Primer sequences were shown in Table 3. Primers were bought from Integrated DNA Technologies Inc (IDT), Coralville IA USA.

## 2.7 Data Analysis

The .cel files were loaded into Partek® Genomics Suite 6.6 (Partek Inc. 2015, St Louis MO) for derivation of quality control metrics to ensure data integrity and validity. Quality control parameters were within normal range as such none of the .cel data was excluded. Data was then subjected to a mixed model analysis of variance (ANOVA). Significantly ($p < 0.05$) differentially expressed genes between control and treated groups and fold change > 2 or fold change < -2 were calculated. False discovery rate (FDR) was 1 %.

Statistical analyses were performed on body and organ weights to assess significant changes in treated groups in comparison to the control animals. Random trend model was employed to test the overall effect from the ingestion of TNDF. All statistical analyses were performed using Statistical Analysis System (SAS) software version 9.3. The data was presented as the mean ± standard error.

# Chapter 3: Results and Discussion

## 3.1 Characterization of $TiO_2$ Nanofibers

Characterization of TDNF was assessed using BET and SEM. Translocation pathways of nanofibers *in vivo* are still not well known. Characterizing the size and shape of ENMs, especially nanofibers, can help ease the way for a more solid understanding ENM translocation. BET data in Figure 1A shows that the surface areas of the fibers were $6.63 m^2/g$. Figure 1B illustrated that not only were the fibers porous, but the fibers contained more smaller pores than larger pores. The length of titanium dioxide nanofibers ranged from 2-50 μm, which was acquired via several SEM images one of which was Figure 2A. These images, in conjunction with the image-j program, were used to determine the diameter of the fibers, which ranged from $45nm \leq x \leq 917nm$ (Figure 3). Recent studies on shape-induced toxicity by titanium dioxide nanofibers have shown a positive relationship on abnormal macrophage morphology with an increase in nanofiber length.[14]

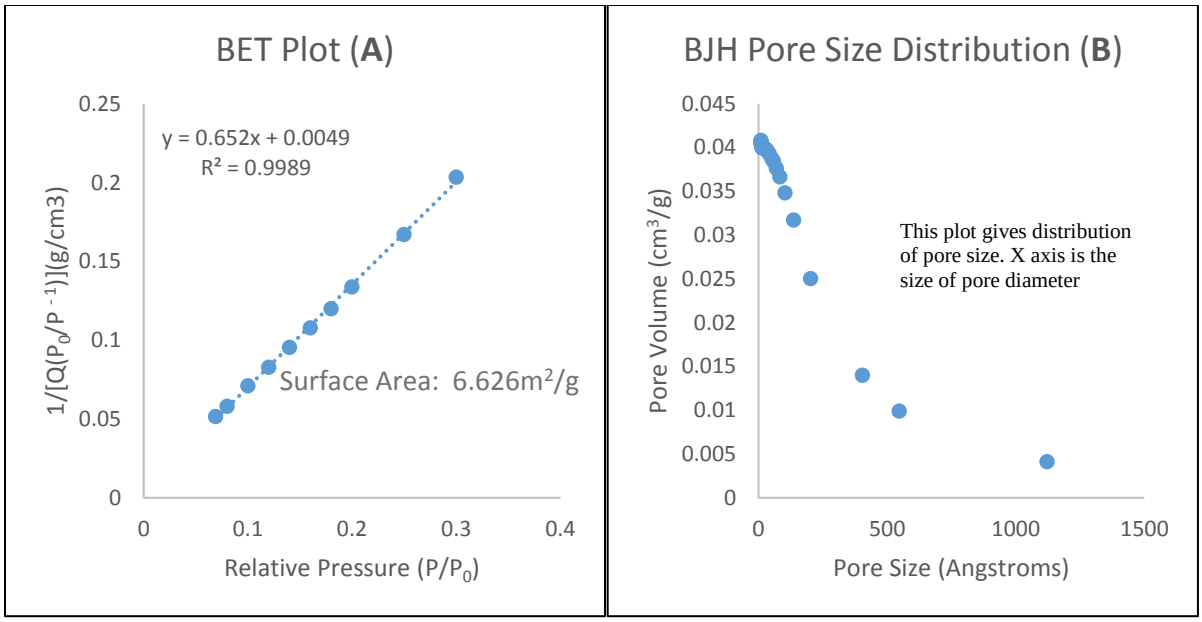


**Figure 1**. Using the equation from the BET Plot (**Left-A**) the surface area for the fibers can be calculated. The BJH Pore Size Distribution (**Right-B**) provides the density of pore sizes within the fibers.

A: $TiO_2$ nano fiber (TNDF) x7000

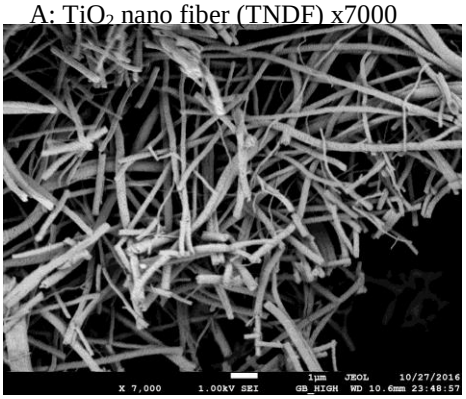


B: $TiO_2$ nano fiber (TNDF) x10000

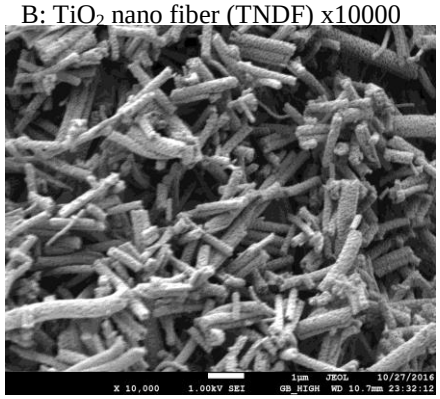


C: $TiO_2$ nano fiber (TNDF) x130000

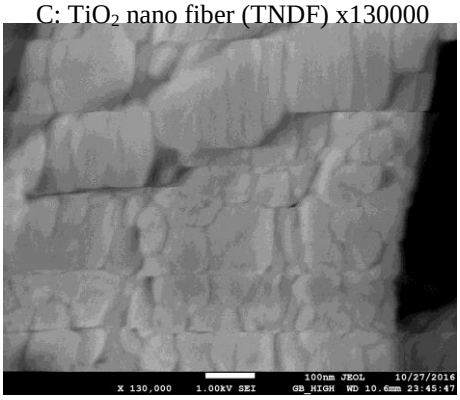


**Figure 2**. SEM images of Purified TDNF at 7000x (A), 10000x (B), and 130000x (C) magnification.

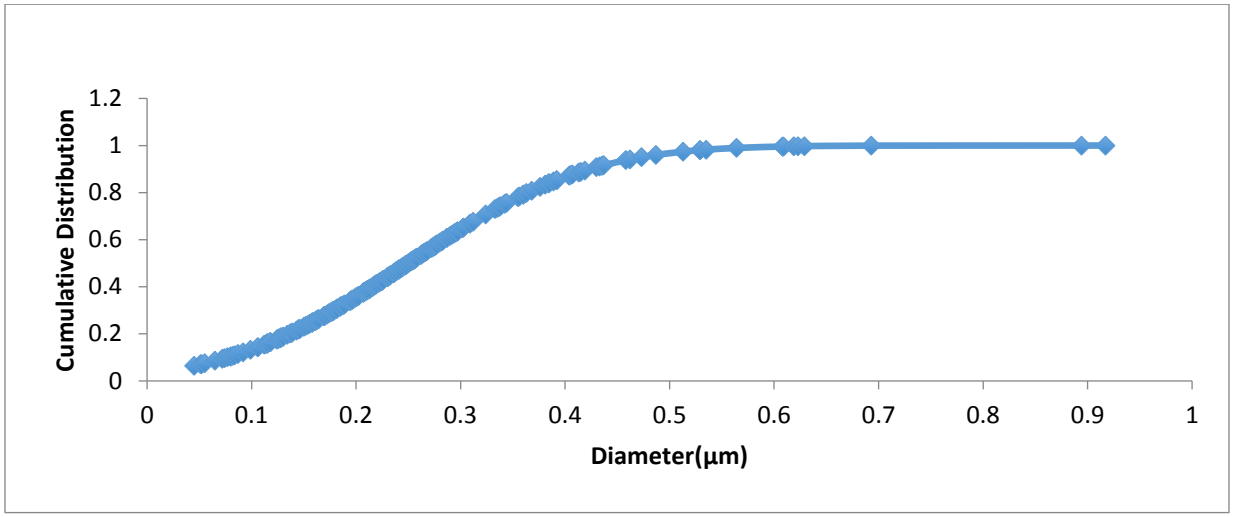


**Figure 3**. Cumulative Distribution of Fiber Diameter acquired through Image J program using various SEM images of the nanofibers.

3.2 TDNF Effect on morphometric indices

There is enough evidence to suggest $TiO_2$ NPs might negatively impact human health. However most of the studies involving $TiO_2$ nanomaterial toxicity comprised *in vitro* models. It is quite a task to make the case for health concerns based solely on cell culture data. In general, exposure to environmental contaminants produces varying effects on body weight gain. Depending on the toxicant, overall body weight can be reduced or significantly increased between control and exposed groups.[15]

The effects of TDNF consumption on amount of diet ingested (Figure 4), weight gain (Figure 5), Feed efficiency (Table 1), and kidney, lung, and liver weights (Figure 6, 7, 8) were measured. The rats were allowed a surplus of food and water to last for 2-3 days. At the end of the 2-3 days the water and food were replenished; the feed was filled to ~200g. Due to natural growth and a sedentary lifestyle the amount of food eaten will increase. Around the second weighing period, according to Figure 4, there is a slight nuance in the difference of cumulative food eaten between the control group and the groups that ingested TDNF (40ppm and 60ppm). However, in the third and fourth weighting periods the difference increases by 60% and then by 90%, with referencing to the second weighting period. There seems to be a small trend in eating habits and ingestion of TDNF; however, there is a lack of supporting evidence from studies showing any such correlation.

The acute effect of TDNF ingest was examined in male Sprague Dawley rats. Exposure to TDNF could result in weight loss. Shown in Figure 5 is the mean weight of the rodents over the course of the study. The overall spaghetti plot showed that all the rats gained weight over time. As anticipated, animals gained weight during treatment. However, the mean weight gain varied depending on the amount of TDNF ingested. At the beginning of the treatment period,

cumulative weight of the control group was least in comparison to the rest. As time went on though, TDNF exposed groups began to reveal slightly reduced weight. By the end of the treatment period, there was a marginal difference between the control animals and TDNF consumed rats.

Feed efficacy (Table 1), the interpretation of how well an animal can convert feed into a desired product was calculated among the three treatment groups; however, the rats were not producing a desired product. Feed efficiency in this study was to see how much feed was converted into body weight. Looking at the FE*100 column of Table 1, among the three treatment groups 50-60% of what was eaten was converted into body weight. However, the differences among the groups was deemed not significant via one-way ANOVA ($F(2,9) = 1.204$, $p= 0.344$).

ENMs have an increased size to surface area ratio. In theory, the nanofibers should be small enough to infiltrate and translocate into various organs via bloodstream. For this reason weight measurement of various organs like the kidney, lungs, and liver were taken. Figure 6 shows the weights of the kidneys of the three treatment groups. The figure depicts a small decrease in average kidney weight as ingestion of TDNF increases. However, the weight change is not significant according to statistical analysis. The weight of the lung was measured after euthanasia. Animals in the control group had the highest mean of lung weight, followed by the medium group rats, with the low concentration TDNF rats showing the lowest lung weights (Figure 7). The weights of the livers, shown in figure 8, were measured on the day of sacrifice. The control group had the highest liver weights followed by the medium group (60ppm) and lastly by the low group (40ppm). At first, it appears that TDNF may have some role in weight loss albeit healthy weight loss or through cytotoxicity. However, upon statistical evaluation

(ANOVA) differences among the three treatment groups are not significant. Furthermore, histopathology rules out any serious tissue damage that would result in weight loss of the liver.

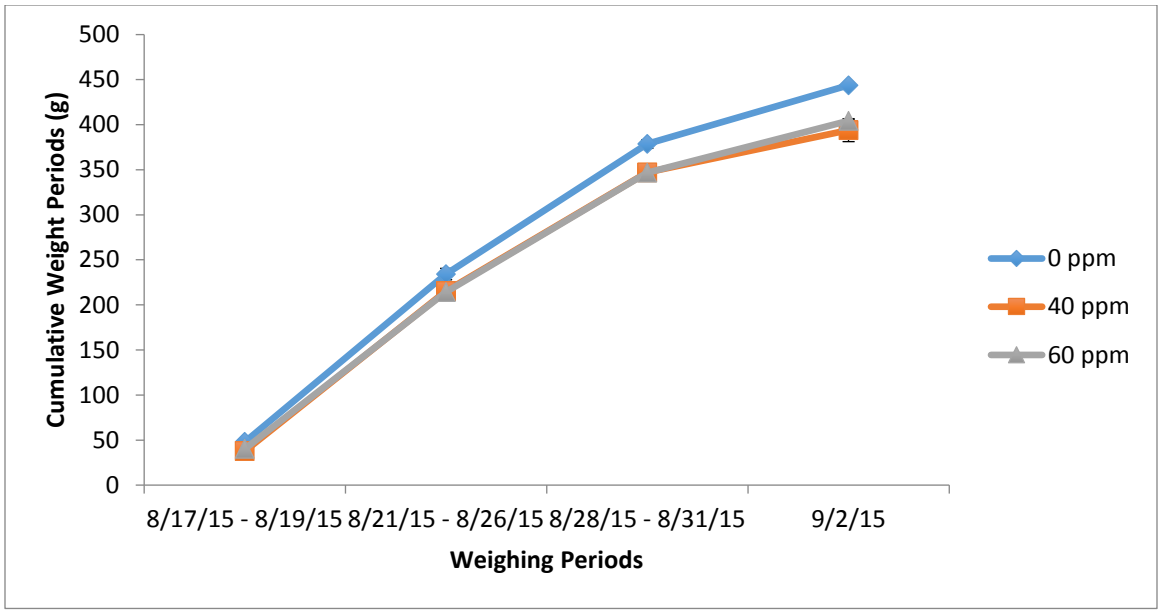


**Figure 4**. Cumulative amount of dietary ingestions over the course of the study. Treated groups seem to consume less of the diet over time.

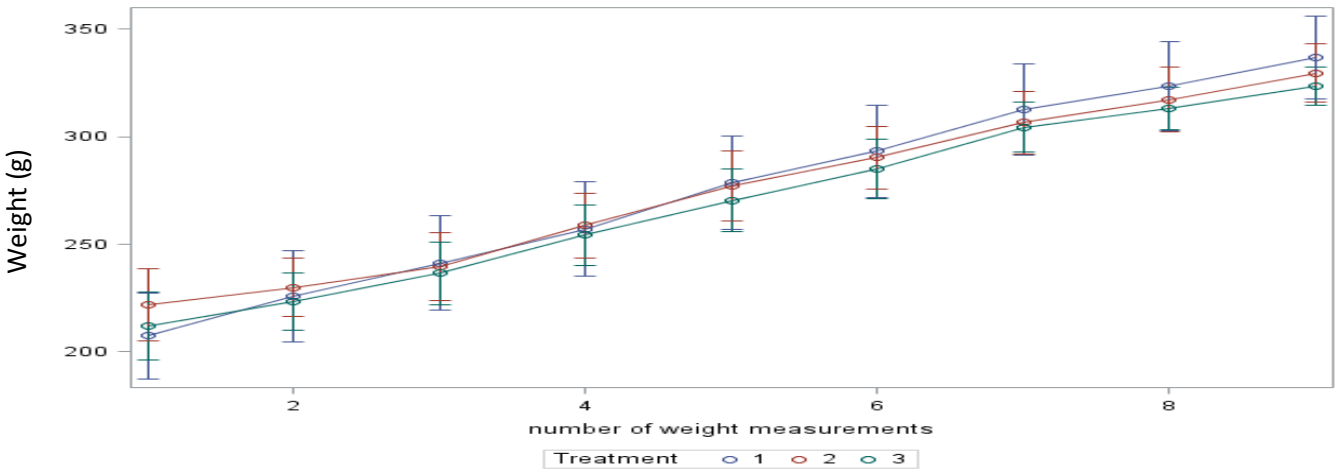


**Figure 5.** Average weight±SE of male Sprague Dawley rats over the course of the study. Weight measurements were performed nine times for two plus weeks. The horizontal axis represents actual weight measurement times. Animals were assigned into dose regimes of treatment 1 (blue – control, 0 ppm); treatment 2 (red – low concentration, 40 ppm) and treatment 3 (green – medium concentration, 60 ppm). Weight gain was not significant.

**Table 1.** Feed Efficiency Data. This figure depicts how well the rodents can convert food consumed into body weight and its significance in the differences between them.

| Treatment Group | Initial Body Weight (g) | Final Body weight (g) | Body weight gain (g) | Gain to Normal Control (%) | Food intake (g) | Feed Efficiency (FE) Value | FE *100 | FE to normal control (%) |
|---|---|---|---|---|---|---|---|---|
| Control | 102.2 ± 24.5 | 336.9 ± 33.3 | 234.7 ± 12.7 | 100.0 | 443.8 ± 22.2 | 0.529 ± 0.016 | 52.9 | 100.0 |
| Low | 103.4 ± 22.0 | 329.7 ± 23.9 | 226.3 ± 13.0 | 96.4 | 394.0 ± 26.9* | 0.578 ± 0.060 | 57.8 | 109.3 |
| Medium | 103.1 ± 22.6 | 323.7 ± 15.4 | 220.7 ± 16.4 | 94.0 | 404.4 ± 10.2* | 0.545 ± 0.027 | 54.5 | 103.0 |

%: relative to control; *: P <0.05 compared with control

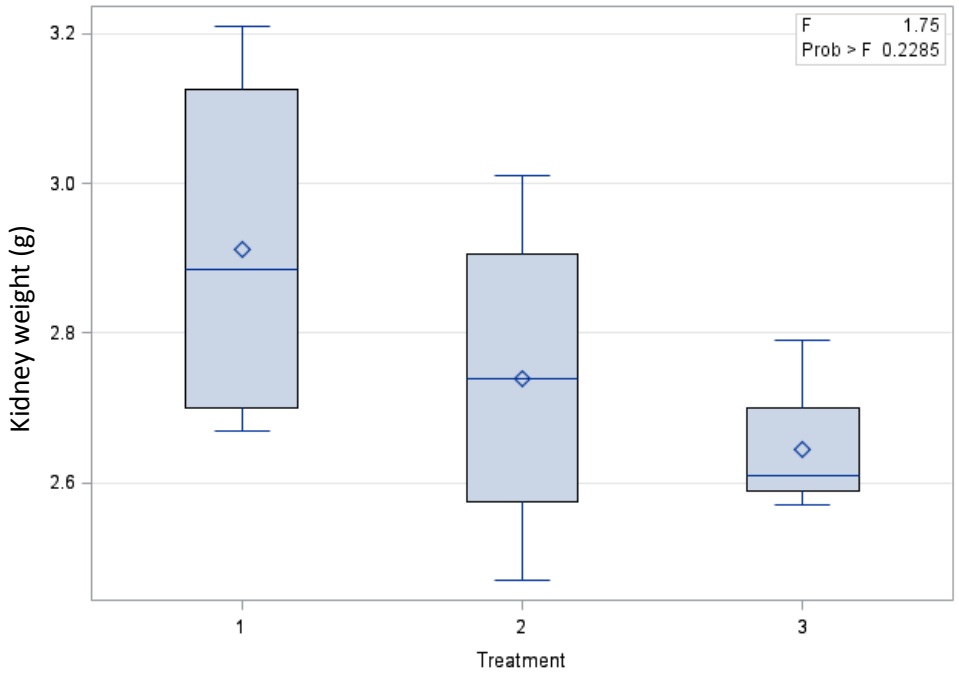


**Figure 6**. Mean kidney weights (g) at the time of sacrifice of rats. Data shown as weight±standard error. Treatments 1, 2 and 3 were 0 ppm; 40 ppm; and 60 ppm $TiO_2$ NF respectively

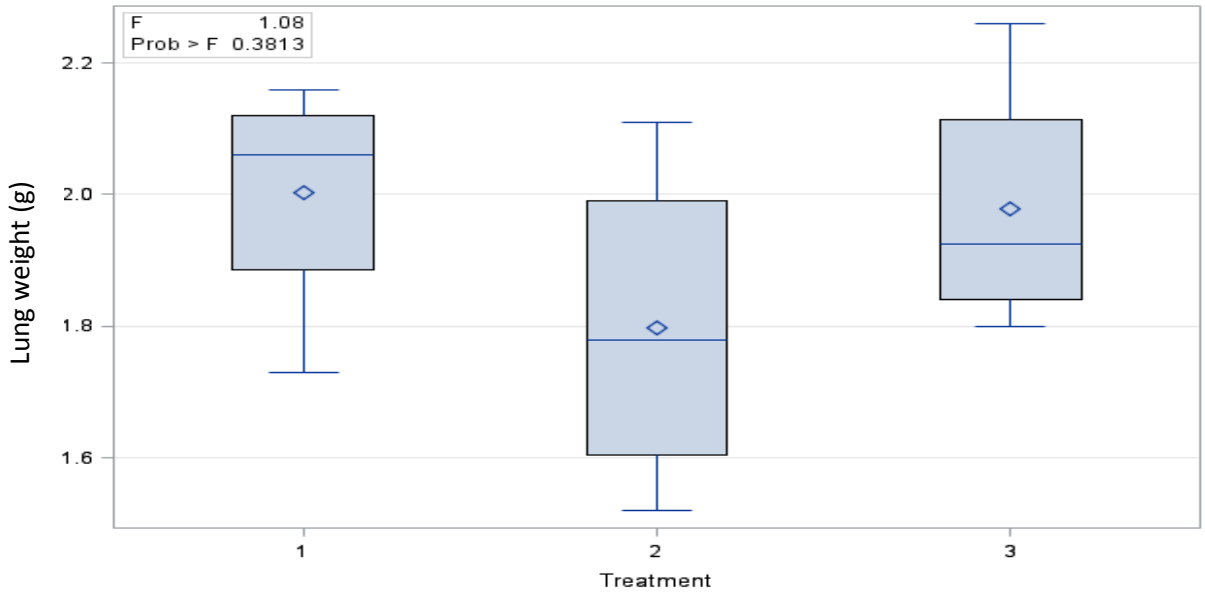


**Figure 7.** Mean lung weights (g) at the time of sacrifice of rats. Data shown as weight±SE. Treatments 1, 2 and 3 were control – 0 ppm, low – 40 ppm, and medium – 60 ppm $TiO_2$ NF respectively.

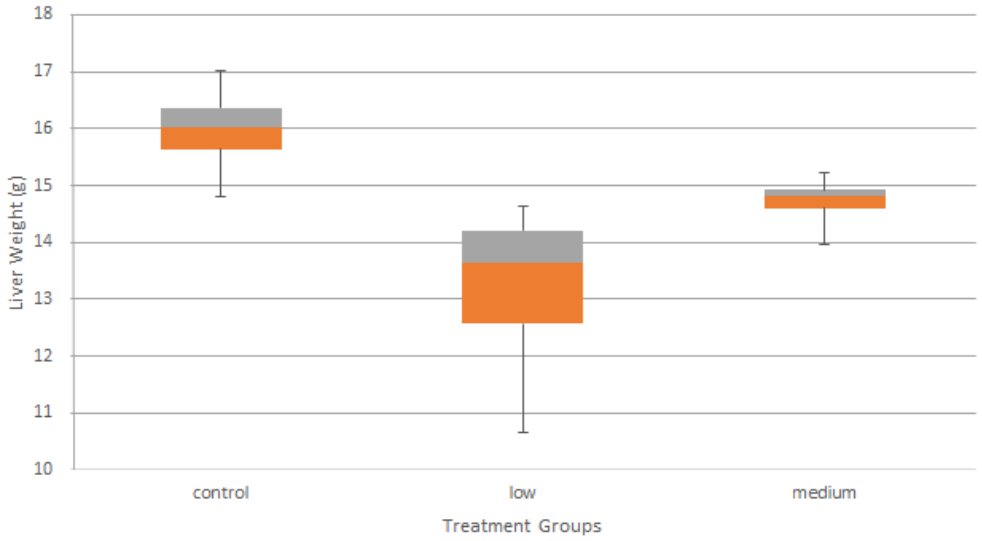


**Figure 8.** Mean Liver weights (g) at the time of sacrifice of rats. Data shown as weight±SE. Control – 0 ppm, low – 40 ppm, and medium – 60 ppm $TiO_2$ NF respectively.

## 3.3 TDNF Effects in the Kidney

### 3.3.1 Histopathology of the Kidney

Kidney tissue was then prepped for histological testing. The trimming and sectioning of the tissue was at a thickness of 4 µm and staining was done with hematoxylin and eosin. The sections were then rated on a scale of 0-3 (0=none, 1-mild, 2= moderate, 3=marked). Assessment kidney histopathology slides were examined. Figure 9 shows no observable morphological irregularities in the renal tissues. However, according to some literature titanium dioxide nanoparticles with sizes of 5 nm or more caused dose dependent inflammatory lesions in rats.[4b] One study injected titanium dioxide nanoparticles into zebra fish and found no damage or trauma to the kidney tissues.[16]

### 3.3.2 Serum Levels of Lactate Dehydrogenase (LDH)

LDH is an enzyme that helps the catalysis of pyruvate into lactate, also converting $NAD^+$ to NADH and back. LDH is released in the presence of damaged cells; therefore, it is used as a marker for tissue injury and diseases. LDH activity in blood serum was significantly elevated in animals exposed to TDNF (Figure 10) in a seemingly concentration-dependent manner. These LDH values ranged from around 450 U/L in the 0 ppm group to over 525 U/L in both the 40 and 60 ppm animals. LDH levels this high should indicate tissue damage; however, histology showed no observable abnormalities in the kidney tissue. High levels aside, there seem to be a dose-dependent relationship between TDNF ingestion between the control group and the treated groups. Statistical analysis tells that the difference in LDH levels between the control and treated groups are not significant.

3.3.3 Selected Inflammatory mRNA Levels in response to TDNF Ingestion

The significant expression of Hepacam2 (Figure 11 panel I) were noted from transcripts previously identified to be responsive to TDNF ingestion in a prior study. On the contrary, CD209, IgG-2a, IghA and RgS13 were not significantly changed in renal tissues. With respect to genes selected based on literature reviews, Gadd45a and NFkB genes were over-expressed in kidney tissues (Figure 11 panel II). Contrarily, IL-1B and TNFalpha seem to be down-regulated relative to 0 ppm groups.

Looking at the 11 genes examined, only 3 showed significant signs of over-expression. NF-KB is a transcription factor that regulates many important pathways such as apoptosis, cell proliferation, pro-/anti-inflammatory processes. Up-regulation of NF-KB could possibly lead to uncontrolled cell death or tumorigenesis, two extreme cases on the opposite sides of cell life. However, this data paired with histology, normal cell counts, and no indication of tumors leads to the assumption that NF-KB was involved with inflammation in the kidneys. However, a typical NF-KB inflammation response should correspond to increased levels of IL-1B and TNFα. Both IL-1B and TNFα help regulate the immune response; therefore, a lack of inflammatory regulation in conjunction with an over-expression of NF-KB should have shown inflammation in the histology slides.

Gadd45a is a protein associated with stressful growth arrest conditions and treatment with DNA-damaging agents. With a small up regulation in both 40 and 60ppm groups, it seems that Ti-47 may have induced stress on the cells. However, lack of upregulation of p21, another major protein associated with cell growth arrest, could indicate cell growth arrest pathway independent of the canonical Gadd45a and p21 pathway. Furthermore, there was no difference in regulation of this pathway according to the static expression of p53 in both low and medium groups.

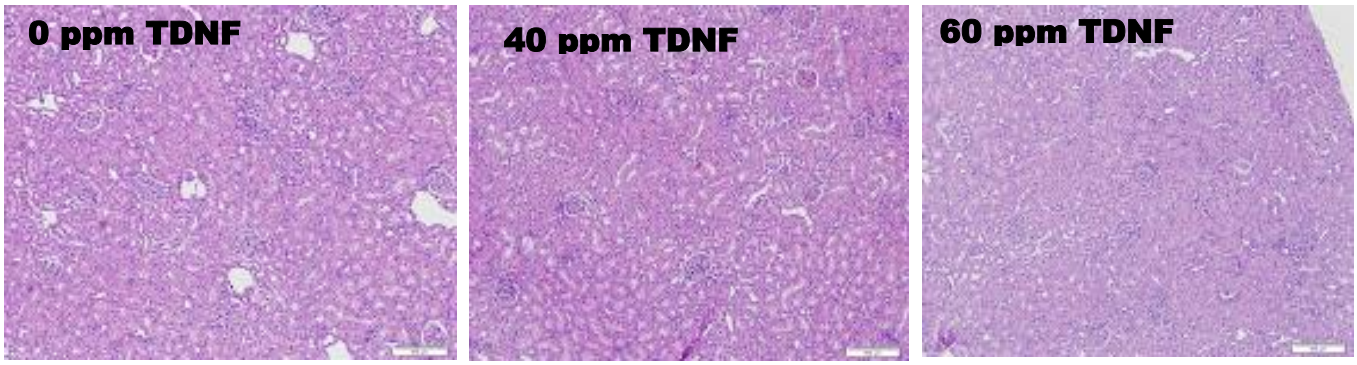


**Figure 9.** Renal anatomic characterization showing select H&E images of male Sprague Dawley rats exposed to 0 ppm (control), 40 ppm (low concentration), 60 ppm (medium concentration) for two weeks via oral gavage.

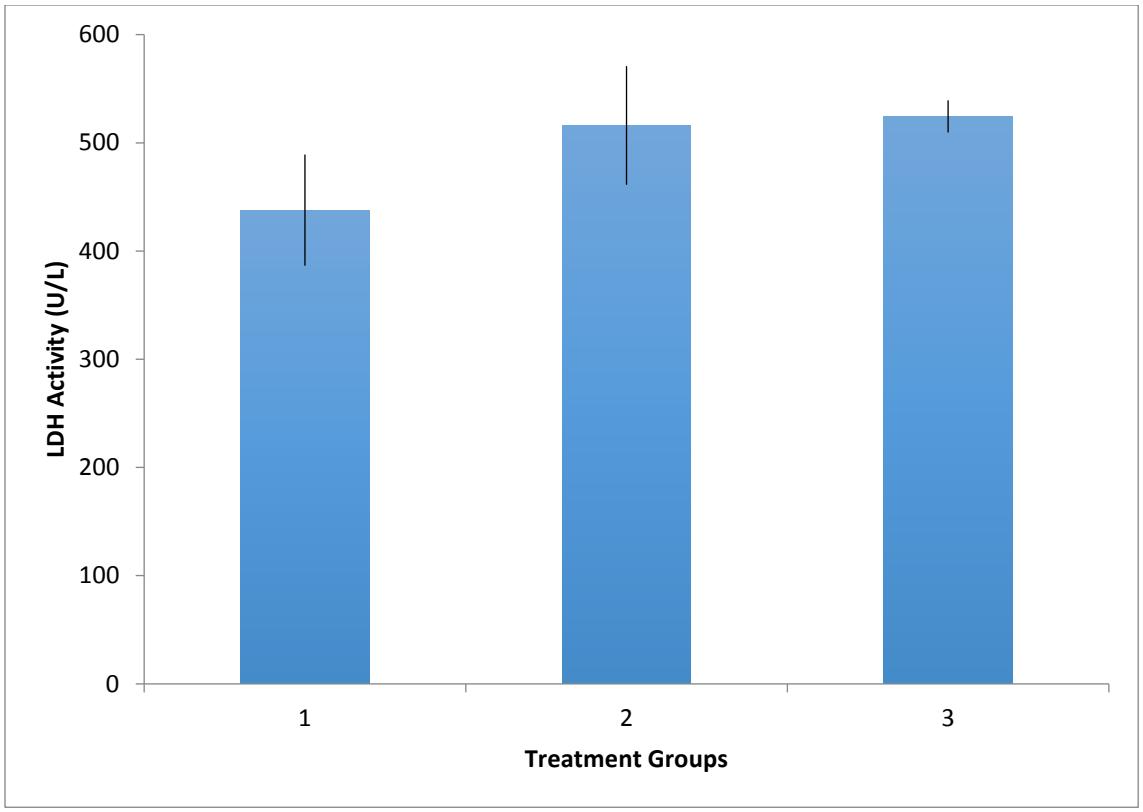


**Figure 10.** Amount of LDH in the serum of animals exposed to TDNF. LDH activity is significantly increased ($p<0.01$) in animals that ingest TDNF. Treated groups were 0ppm, 40 ppm, 60 ppm TDNF.

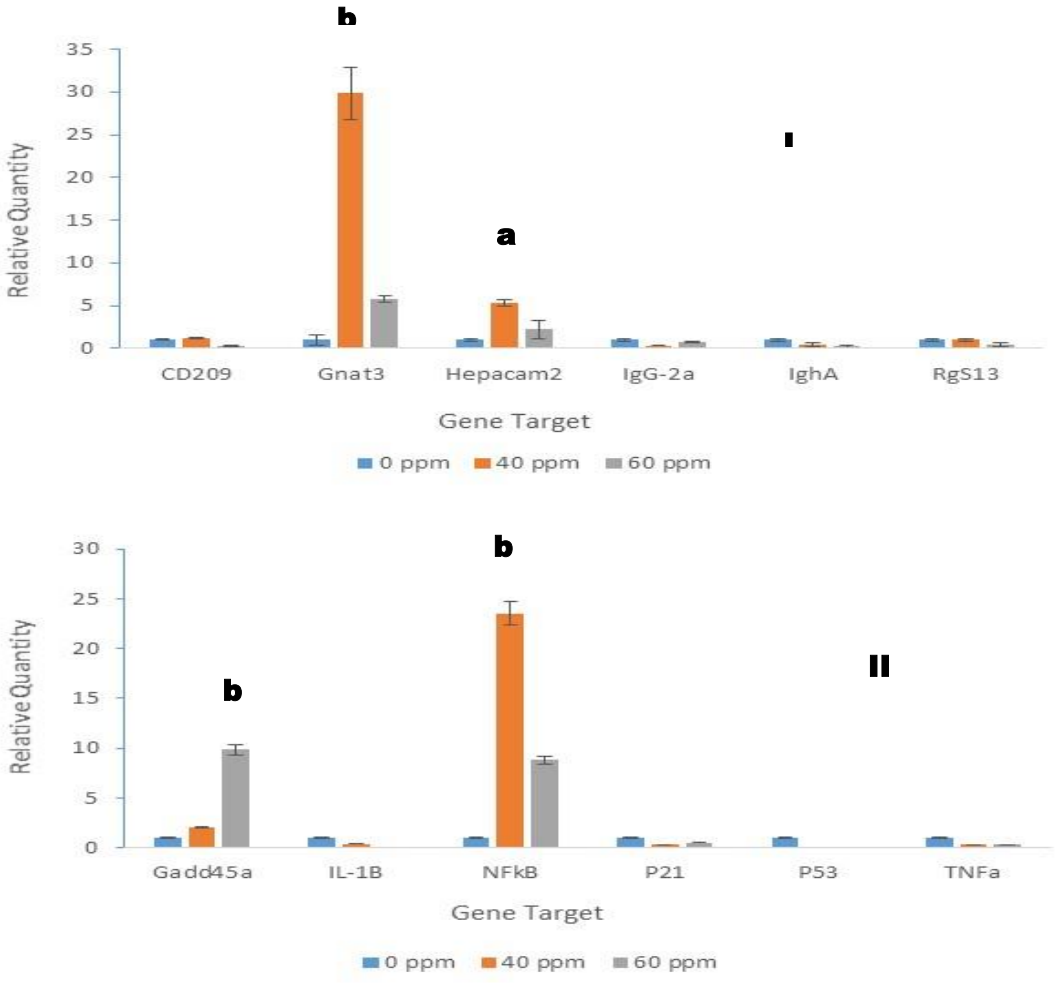


**Figure 11.** The relative mRNA expression (ΔCq) of a select genes in the kidneys of rats that ingested TDNF at 0 ppm (control – FC); 40 ppm (low concentration – FLC) and 60 ppm (medium concentration – FMC). Gnat3 and and Hepacam2 were differentially expressed. Significant changes were noted as $^{a}P<0.05$, $P>0.01$. Panel I shows genes previously identified from a study in our laboratory. Panel genes were identified in the literature to be responsive to TDNF in other systems

## 3.4 TDNF Effects in the Liver

### 3.4.1 Histopathology of the Liver

The H&E staining of the tissues showed no considerable differences among the three treatment groups, with respect to liver damage.

### 3.4.2 Serum Levels of Alanine Aminotransferase and Albumin

Serum levels, specifically albumin (ALB) and alanine aminotransferase (ALT), are excellent indicators of liver health. Small deviations in the amount of ALB in liver tissue could mean that the liver were functioning as expected as ALB levels can vary depending on food consumption; however, large variation of albumin could indicate damage. Likewise, an increase in the amount of ALT could indicate liver damage. Serum levels of alanine aminotransferase (ALT) of the control group were substantially higher than those from reference values. When comparing the serum levels among the three groups there is a dose dependent relationship in increased TDNF ingestion with decreased ALT levels. The decreased ALT activity in the treated groups; however, bring the levels within reference values. This could be due to possible serum contamination from fat cell aggregates or possible cell layer contamination. When looking at the three groups ANOVA indicated that differences in the ALT activity were significant ($p$-value$<0.01$).

Albumin levels in the control and low groups were within one standard deviation of the literature value ($4.4 \pm 0.5$). The ALB levels, in the medium dose group, were not statistically significant with respect to the reference value (Table 2). It is worth noting that the low dose group was statistically different from the control and medium groups ($p=0.0012$). However, Table 2 clearly shows that albumin levels coincide with literature values for rodents. On the

other hand, ALT levels are extremely high compared to reference values, which could be interpreted as liver damage.

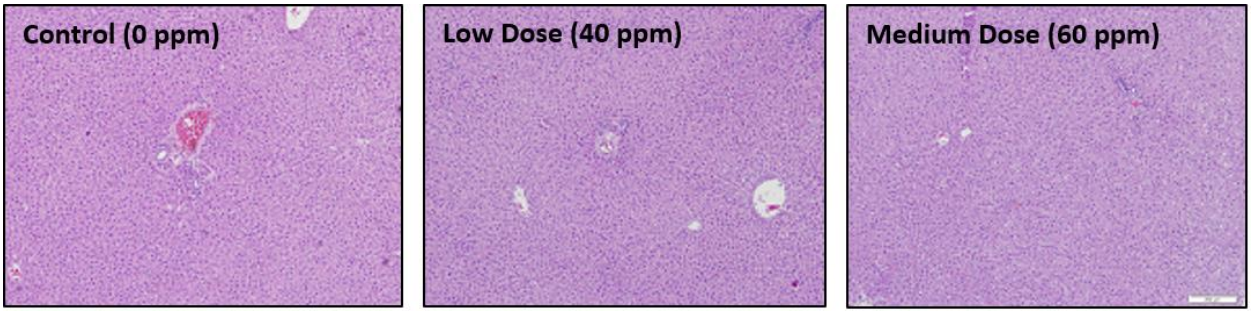


**Figure 12**. Images of hepatic cells taken from livers of rats in the control (0 ppm TDNF), low dose (40 ppm TDNF), and medium dose (60 ppm TDNF) groups.

**Table 2**. Concentration of ALT and ALB in the control (0 ppm TDNF), low (40 ppm TDNF), and medium (60 ppm TDNF) exposure groups. Reference values are for ALT and ALB levels in serum of female rats between 8 and 16 weeks old.[17]

| | Reference Mean ± SD | control | low | medium |
|---|---|---|---|---|
| [ALT] U/L | 25 ± 9 | 48.05 ± 1.33 | 22.04 ± 2.37 | 19.50 ± 2.38 |
| [ALB] g/dL | 4.4 ± 0.5 | 3.92 ± 0.042 | 4.47 ± 0.094 | 3.73 ± 0.17 |

**Table 3.** Primer sequences of the 11 genes studied.

| Gene Name | Primer Sequence | |
|---|---|---|
| CD209 | Forward | 5'CTCCAAATCCCAGCGTAACT3' |
| | Reverse | 5'ACAGCAGAGGTCAAGGAAAC3' |
| Igha | Forward | 5'TCTGGACCTGAACTGGAGAA3' |
| | Reverse | 5'TGGGTAGATGGTGGGATCTT3' |
| IgG-2a | Forward | 5'GCCTGGTCAAGGGCTATTT3' |
| | Reverse | 5'GTAACTCCCATCTGTGTCCATC3' |
| Hepacam2 | Forward | 5'GACTGTTCTGCTGACTCTTATCC3' |
| | Reverse | 5'CTCTGTGTCGTCTTGCTGTT3' |
| Rgs13 | Forward | 5'GTACAACACGGGAAGCTATCA3' |
| | Reverse | 5'TAATCATGGGCGTGCTACAG3' |
| TNF-α | Forward | 5'ACAAGGCTGCCCCGACTAT3' |
| | Reverse | 5' CTCCTGGTATGAAGTGGCAAATC3' |
| IL-1β | Forward | 5' TACCTATGTCTTGCCCGTGGAG3' |
| | Reverse | 5' ATCATCCCACGAGTCACAGAGG3' |
| NF-kB | Forward | 5' AGCAGGATGCTGAGGATTCTG3' |
| | Reverse | 5' GGCAACTCTGTCCTGCACCTA3' |
| P53 | Forward | 5'GTGGCCTCTGTCATCTTCCG3' |
| | Reverse | 5' CCGTCACCATCAGAGCAACG3' |
| P21 | Forward | 5' AGCAAAAGAGGCAACCAAGA3' |
| | Reverse | 5' GGGTAAGGAATGGGATGGTT3' |
| Gadd45-α | Forward | 5' GGAAGCTGCGAGAAAAGAGA3' |
| | Reverse | 5' TGAAAGTAACCTGGCCATCC3' |

## 3.5 TDNF Effects in the Lung

### 3.5.1 Histopathology of the Lung

Lung samples were fixed in 10% neutral buffered formalin for at least 48 hours, trimmed, routinely processed for histology, sectioned at 4-µm thickness, and stained with hematoxylin and eosin. Histologic changes were evaluated subjectively on a scale from 0 to 3, with 0=none, 1=mild, 2=moderate, and 3=marked.

Pathological assessment of the lung is shown in Figure 13. Anatomical evaluation showed no significant changes between the animals that ingested TDNF and control groups.

### 3.5.2 Serum Total Protein

Significant reductions in total protein concentration in animals that ingested TNDF in comparison to the control groups (Figure 14). Serum total protein concentration was significantly reduced in animals that ingested TDNF. During the course of the experiment the Total Protein of the lungs was analyzed. The total protein test quantifies the amount of albumin and globulins in the blood vessels, which are responsible for preventing leaks and helping the immune system, respectively. Thus, any deviation from normal or expected total protein concentrations can prove detrimental to the tissue and even the organism. When looking at the total protein graph one can tell that there is a decrease in total protein when comparing the control groups to the treated groups. There is also a slight decrease in the total protein amount when comparing the medium dose group to the low dose group.[18]

3.5.3 Assessing Genome-wide Effect of TNDF

Additional adverse effects were examined in the genome-wide mRNA expression of the lung. The goal was to assess the differential expression of unique gene transcripts in the lung. Volcano plot of differentially expressed that were at least 2-fold up- or down-regulated are represented in Figure 15. Blue or red dots indicate a gene. Up- and down-regulated genes were those falling outside of the pair of marker lines of fold change of -2 to +2 as seen in Figure 15A, B & C. Numbers of transcripts decoded from Figure 15 is plotted as a Venn diagram in Figure 16. Rats that ingested more TNDF also had a higher number of differentially expressed transcripts. Comparison of the control group and 40 ppm-treatment group showed 39 significantly changed transcripts. The comparison of the control group to the 60 ppm treatment group and the comparison of the 40 ppm treatment group to the 60 ppm treatment group showed 58 and 57 significantly changed genes, respectively.

The differentially expressed genes within the TNDF treated groups seem to play essential roles in cellular immunity. Some of these include; CD209 antigen-like protein, immunoglobulin heavy chain alpha, and hepacam2 (immunoglobulin superfamily of cell adhesion molecules) (Table 4). Cd209 is reported to be crucial for modulating endogenous glycoprotein clearance.[19] Both treatment groups indicate an over-expression of immunoglobulin heavy chain, alpha (Igha) transcript. This particular gene is vital for immune responses. It blocks viral attachment as well as neutralizing virus infectivity.[20] From the preceding, one can deduce that the fibers are too long to penetrate the cell, however they may serve as a phagocytosis site at the point of deposit that can lead to inflammation.

Mapping of significantly changed genes onto pathways may be important to understand the adverse effects associated with TDNF exposure (Table 5). Several pathways from KEGG

were identified to be relevant to assessing the toxicity of TNDF. Some of these are TNF signaling pathway, Cytokine-cytokine receptor interaction, cAMP signaling pathway, MAPK signaling pathway, chemokine signaling pathway and inflammatory mediator regulation of TRP channels.

### 3.5.4 Igha mRNA Levels in response to TDNF Ingestion

Clinical chemistry and morphometric indices can provide insightful knowledge regarding the short-term effect of TDNF ingestion. Nevertheless noting changes at the molecular level via these techniques will not be apparent. Global gene expression analysis provides the opportunity to examine transcriptional modifications in biological systems.[21] This will provide an understanding of toxic effects at the molecular level.

Quantitative measurement of IgA (immunoglobulin A) was undertaken in lungs as a way to validate microarray data. IgA is the principal line of defense against pathogens and other foreign materials.[22] The Ig heavy chain alpha has been reported to play crucial roles in cellular transcription and recombination.[23] To assess the validity of broad gene expression patterns, the Igha transcript was quantified in lung tissues.

Genome-wide differential gene expression data was validated using quantitative PCR analysis of the Igha gene. Global gene expression data showed that Igha was down-regulated in the low concentration group while up-regulated in the 60ppm treated group. However the qPCR data indicated that Igha mRNA was over-expressed in the FLC and FMC treated rats compared with control groups (Figure 17). Still the medium concentration animals expressed higher levels of the Igha than the low concentration group. A study a few years ago assessing the toxicity of subchronic exposure to TCDD (2, 3, 7, 8-Tetrachlorodibenzo-p-dioxin) found Igha was down-

regulated in the liver of rats.[24] Another study recently revealed that airways proteins such as Igha (IgA constant region) was found to be affected by exposure to glutathione reaction product and methylene-diphenyl diisocyanate (MDI).[25]

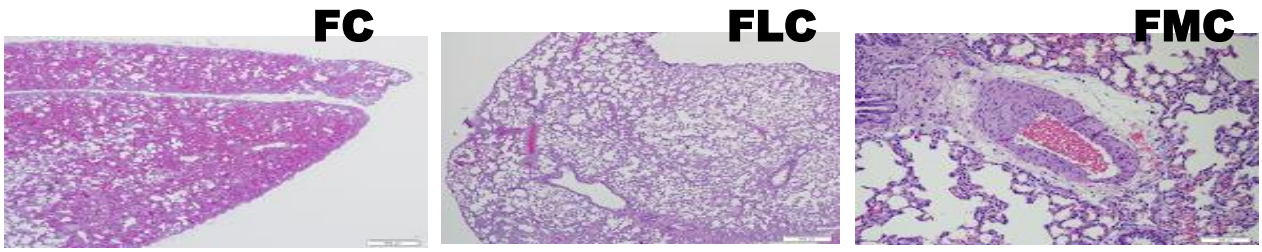


**Figure 13.** Anatomic characterization of select H&E images of lungs of male Sprague Dawley rats exposed to 0 ppm (FC), 40 ppm (FLC), and 60 ppm (FMC) for two weeks via oral gavage.

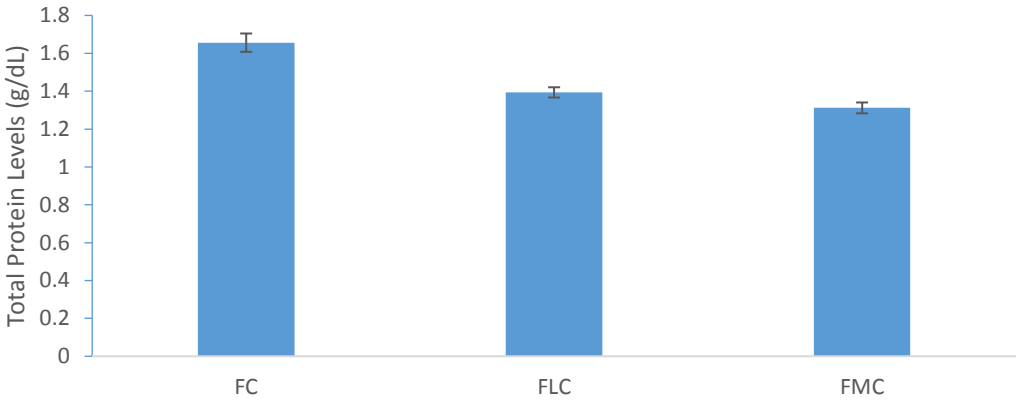


**Figure 14.** Total protein concentration in the serum of Sprague Dawley rats ingested 0 ppm (FC), 40 ppm (FLC) and 60 ppm (FMC) Titanium Dioxide Nanofibers for two weeks. Total Protein levels were significantly ($p<0.05$) reduced in rats that ingested TDNF.

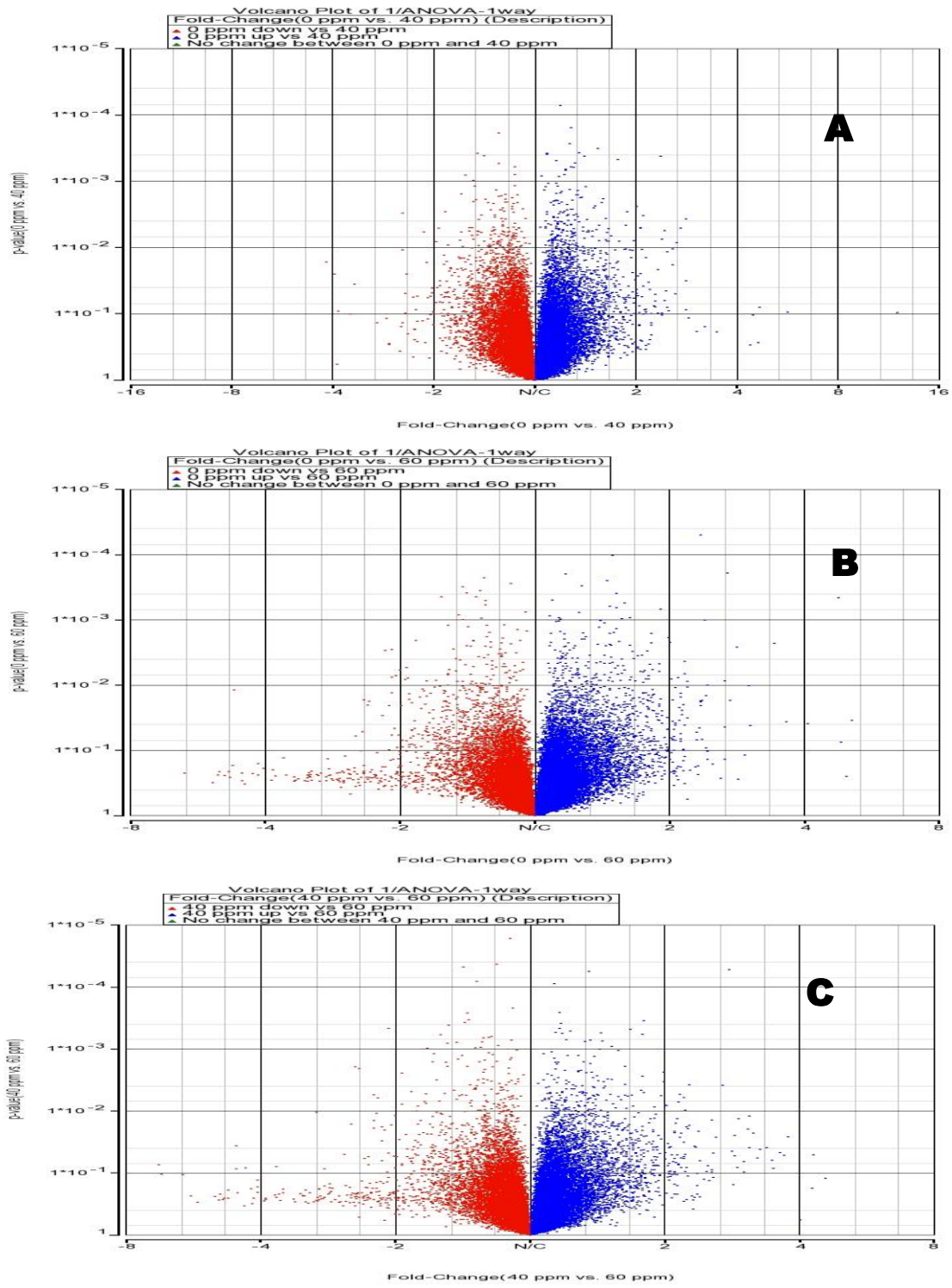


**Figure 15.** Volcano plot of lung differentially expressed genes from TDNF exposed rodents. The plot of p-value relative to fold-change shows comparison between control and treated groups; A) control vs low concentration (40 ppm), and control vs medium concentration (60 ppm).

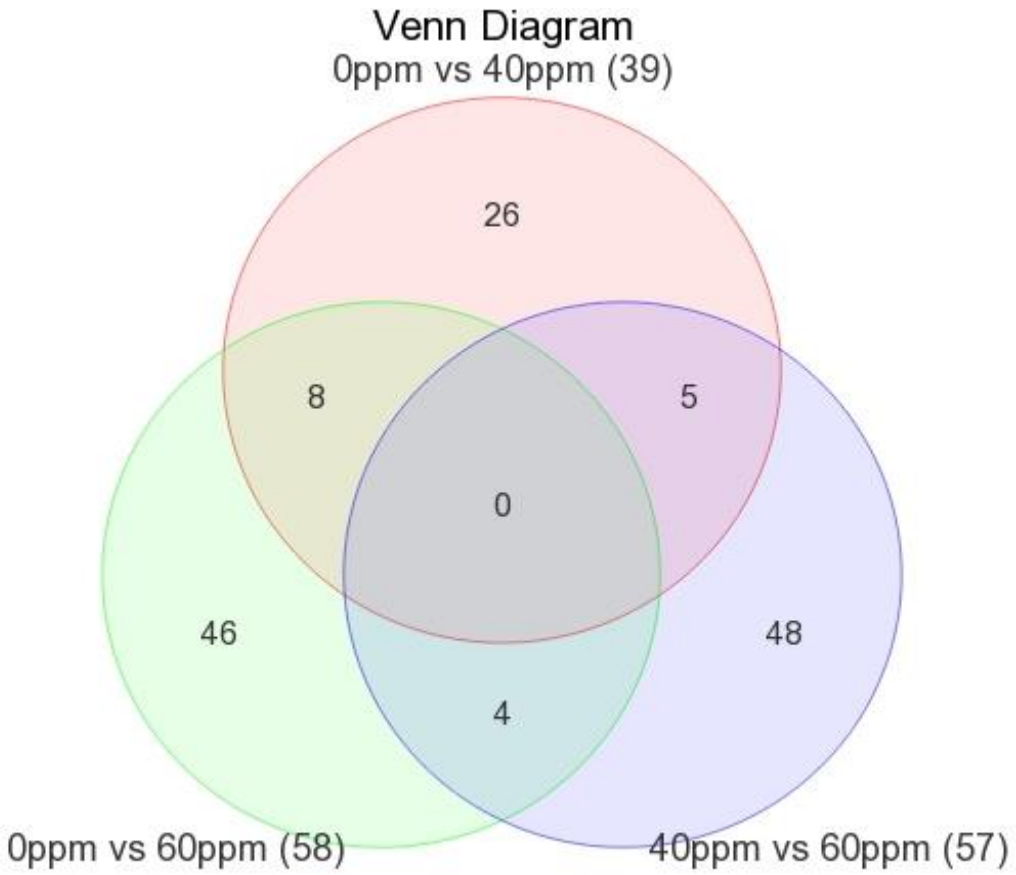


**Figure 16.** Venn diagram shows connection of significantly ($p<0.05$) altered genes between groups. Comparing 0ppm vs 40ppm showed a total of 39 genes differentially expressed while 0ppm vs 60ppm and 40ppm vs 60ppm indicated 58 and 57 transcripts respectively. There were no common gene expressed in all three of the groups.

**Table 4.** Select number of altered mRNA transcripts between the groups. These genes were extracted from Figure 2A which showed 16 genes to be common to all dose regimes.

| Control vs 40ppm Treatment Group | | | | | |
|---|---|---|---|---|---|
| Gene_assignment | Gene Symbol | p-value(0 ppm vs. 40 ppm) | Ratio(0 ppm vs. 40 ppm) | Fold-Change(0 ppm vs. 40 ppm) | Fold-Change(0 ppm vs. 40 ppm) (Description) |
| XM_003752548 // LOC100912723 // CD209 antigen-like protein A-like // --- // 100912723 | LOC100912723 | 0.0109 | 0.402987 | -2.48147 | 0 ppm down vs 40 ppm |
| XM_006221059 // LOC102551003 // keratin-associated protein 20-2-like // --- // 10255100 | LOC102551003 | 0.0106 | 2.082 | 2.082 | 0 ppm up vs 40 ppm |
| BC087057 // Igha // immunoglobulin heavy chain, alpha // 6q32 // 314487 | Igha | 0.0356 | 0.290157 | -3.4464 | 0 ppm down vs 40 ppm |
| NM_001191973 // Ccdc129 // | Ccdc129 | 0.0405 | 0.492741 | -2.02947 | 0 ppm down vs 40 ppm |
| Control vs 60ppm Treatment Group | | | | | |
| Gene_assignment | Gene Symbol | p-value(0 ppm vs. 40 ppm) | Ratio(0 ppm vs. 40 ppm) | Fold-Change(0 ppm vs. 40 ppm) | Fold-Change(0 ppm vs. 40 ppm) (Description) |
| ENSRNOT00000039185 // Hps5 // Hermansky-Pudlak syndrome 5 // 1q22 // 308598 /// ENSRNOT | Hps5 | 0.0042 | 2.15772 | 2.15772 | 0 ppm up vs 60 ppm |
| ENSRNOT00000048829 // RGD1564184 // similar to monoclonal antibody 17-1A, light chain / | RGD1564184 | 0.0099 | 2.43501 | 2.43501 | 0 ppm up vs 60 ppm |
| FQ234364 // IgG-2a // gamma-2a immunoglobulin heavy chain // 6q32 // 367586 | IgG-2a | 0.0197 | 2.14326 | 2.14326 | 0 ppm up vs 60 ppm |
| ENSRNOT00000038646 // Igl // | Igl | 0.0342 | 5.09259 | 5.09259 | 0 ppm up vs 60 ppm |
| 40ppm vs 60ppm Treatment Group | | | | | |
| Gene_assignment | Gene Symbol | p-value(0 ppm vs. 40 ppm) | Ratio(0 ppm vs. 40 ppm) | Fold-Change(0 ppm vs. 40 ppm) | Fold-Change(0 ppm vs. 40 ppm) (Description) |
| NM_001106580 // Hepacam2 // HEPACAM family member 2 // 4q13 // 296846 /// ENSRNOT000000 | Hepacam2 | 0.0071 | 2.15206 | 2.15206 | 40 ppm up vs 60 ppm |
| XM_003752548 // LOC100912723 // CD209 antigen-like protein A-like // --- // 100912723 | LOC100912723 | 0.0180 | 2.23899 | 2.23899 | 40 ppm up vs 60 ppm |
| NM_173139 // Gnat3 // guanine nucleotide binding protein, alpha transducing 3 // 4q11 / | Gnat3 | 0.0081 | 2.02105 | 2.02105 | 40 ppm up vs 60 ppm |
| XM_001068656 // Rgs13 // | Rgs13 | 0.0120 | 3.09498 | 3.09498 | 40 ppm up vs 60 ppm |
| NM_053333 // Retnla // resistin like alpha // | Retnla | 0.0131 | 2.93234 | 2.93234 | 40 ppm up vs 60 ppm |
| XM_006255431 // LOC685226 // | LOC685226 | 0.0170 | 2.26691 | 2.26691 | 40 ppm up vs 60 ppm |
| XM_002727416 // LOC685989 // | LOC685989 | 0.0190 | 2.25025 | 2.25025 | 40 ppm up vs 60 ppm |
| XM_006255431 // LOC685226 // | LOC685226 | 0.0212 | 2.3786 | 2.3786 | 40 ppm up vs 60 ppm |
| BC087057 // Igha // | Igha | 0.0413 | 3.27428 | 3.27428 | 40 ppm up vs 60 ppm |
| NM_017146 // Mcpt10 // | Mcpt10 | 0.0261 | 3.77258 | 3.77258 | 40 ppm up vs 60 ppm |
| XM_006227158 // LOC679730 // | LOC679730 | 0.0379 | 2.34971 | 2.34971 | 40 ppm up vs 60 ppm |
| XM_006227158 // LOC679730 // | LOC679730 | 0.0368 | 2.32343 | 2.32343 | 40 ppm up vs 60 ppm |

| | | | | | |
|---|---|---|---|---|---|
| XM_003748679 // LOC501467 // s | LOC501467 | 0.0388 | 3.38318 | 3.38318 | 40 ppm up vs 60 ppm |
| NM_001108388 // Scel // sciellin // | Scel | 0.0364 | 0.220588 | -4.53334 | 40 ppm down vs 60 ppm |
| XM_003748679 // LOC501467 // | LOC501467 | 0.0387 | 3.09909 | 3.09909 | 40 ppm up vs 60 ppm |
| XM_006255043 // LOC689453 // | LOC689453 | 0.0465 | 3.63195 | 3.63195 | 40 ppm up vs 60 ppm |
| XM_003748679 // LOC501467 // | LOC501467 | 0.0441 | 2.8232 | 2.8232 | 40 ppm up vs 60 ppm |
| XM_003751851 // LOC679730 // | LOC679730 | 0.0472 | 2.57289 | 2.57289 | 40 ppm up vs 60 ppm |

**Table 5.** Pathways assessed to be significantly ($p<0.05$) altered by oral ingestion of TDNF using KEGG (Kyoto Encyclopedia of Genes and Genomes). Percentage of genes involved in each pathway ranged from 97 to 103.

| Pathway Name | Enrichment Score | Enrichment p-value | % genes in pathway that are present | # genes in list, in pathway |
|---|---|---|---|---|
| cAMP signaling pathway | 9.87006 | 5.17E-05 | 100.518 | 194 |
| Adrenergic signaling in cardiomyocytes | 7.37151 | 0.000629 | 101.399 | 145 |
| FoxO signaling pathway | 6.72035 | 0.001206 | 100 | 133 |
| Chemokine signaling pathway | 6.59099 | 0.001373 | 99.4318 | 175 |
| Cytokine-cytokine receptor interaction | 6.54372 | 0.001439 | 99.0654 | 212 |
| Hepatitis C | 6.15986 | 0.002113 | 100 | 122 |
| Sphingolipid signaling pathway | 6.10895 | 0.002223 | 100 | 121 |
| Protein processing in endoplasmic reticulum | 6.08662 | 0.002273 | 99.3939 | 164 |
| Thyroid hormone signaling pathway | 5.90538 | 0.002725 | 100 | 117 |
| Oxytocin signaling pathway | 5.67723 | 0.003423 | 99.359 | 155 |
| Oocyte meiosis | 5.62983 | 0.003589 | 101.835 | 111 |
| Insulin resistance | 5.60023 | 0.003697 | 100 | 111 |
| Cholinergic synapse | 5.54939 | 0.00389 | 100 | 110 |
| TNF signaling pathway | 5.39694 | 0.00453 | 100 | 107 |
| Chagas disease (American trypanosomiasis) | 5.14298 | 0.00584 | 100 | 102 |
| Rap1 signaling pathway | 5.09067 | 0.006154 | 98.5915 | 210 |
| PI3K-Akt signaling pathway | 5.04025 | 0.006472 | 97.8979 | 326 |
| Choline metabolism in cancer | 5.00387 | 0.006712 | 101.02 | 99 |
| Signaling pathways regulating pluripotency of stem cells | 4.9129 | 0.007351 | 99.2806 | 138 |
| Phosphatidylinositol signaling system | 4.90211 | 0.007431 | 101.042 | 97 |
| Melanogenesis | 4.83845 | 0.007919 | 100 | 96 |
| Circadian entrainment | 4.78773 | 0.008331 | 100 | 95 |
| Estrogen signaling pathway | 4.74952 | 0.008656 | 101.075 | 94 |
| Toll-like receptor signaling pathway | 4.68629 | 0.009221 | 100 | 93 |
| Glycerophospholipid metabolism | 4.68629 | 0.009221 | 100 | 93 |
| cGMP-PKG signaling pathway | 4.66842 | 0.009387 | 98.8166 | 167 |
| Proteoglycans in cancer | 4.59698 | 0.010082 | 98.5 | 197 |
| Neuroactive ligand-receptor interaction | 4.51988 | 0.01089 | 97.9167 | 282 |
| GnRH signaling pathway | 4.4835 | 0.011294 | 100 | 89 |
| Progesterone-mediated oocyte maturation | 4.39373 | 0.012355 | 101.163 | 87 |
| Prostate cancer | 4.39373 | 0.012355 | 101.163 | 87 |
| Axon guidance | 4.38141 | 0.012508 | 99.2126 | 126 |
| Dopaminergic synapse | 4.38141 | 0.012508 | 99.2126 | 126 |
| Endocytosis | 4.36019 | 0.012776 | 97.8799 | 277 |

| | | | | |
|---|---|---|---|---|
| MAPK signaling pathway | 4.35599 | 0.01283 | 98.0315 | 249 |
| Insulin secretion | 4.29213 | 0.013676 | 101.19 | 85 |
| TGF-beta signaling pathway | 4.1398 | 0.015926 | 101.235 | 82 |
| Hippo signaling pathway | 4.02961 | 0.017781 | 98.6928 | 151 |
| Calcium signaling pathway | 3.89601 | 0.020323 | 98.3425 | 178 |
| Glutamatergic synapse | 3.77121 | 0.023024 | 99.115 | 112 |
| Prolactin signaling pathway | 3.73386 | 0.0239 | 101.37 | 74 |
| Pathways in cancer | 3.71438 | 0.024371 | 97.2152 | 384 |
| Inflammatory mediator regulation of TRP channels | 3.68501 | 0.025097 | 99.0991 | 110 |
| Gastric acid secretion | 3.62288 | 0.026706 | 100 | 72 |
| Melanoma | 3.58176 | 0.027827 | 101.429 | 71 |
| Bile secretion | 3.53107 | 0.029274 | 101.449 | 70 |
| Ras signaling pathway | 3.51735 | 0.029678 | 97.807 | 223 |
| Thyroid hormone synthesis | 3.47121 | 0.031079 | 100 | 69 |
| Renin secretion | 3.37904 | 0.03408 | 101.515 | 67 |
| Glioma | 3.28637 | 0.037389 | 103.175 | 65 |
| Fc epsilon RI signaling pathway | 3.27773 | 0.037714 | 101.563 | 65 |
| Amphetamine addiction | 3.27773 | 0.037714 | 101.563 | 65 |
| Long-term potentiation | 3.23559 | 0.039337 | 103.226 | 64 |
| Pancreatic cancer | 3.22708 | 0.039673 | 101.587 | 64 |
| Synaptic vesicle cycle | 3.11757 | 0.044265 | 100 | 62 |
| Glucagon signaling pathway | 3.0894 | 0.045529 | 98.9691 | 96 |
| Taste transduction | 3.06708 | 0.046557 | 100 | 61 |
| Pancreatic secretion | 3.04742 | 0.047481 | 98.9583 | 95 |
| AMPK signaling pathway | 3.03243 | 0.048198 | 98.4252 | 125 |
| VEGF signaling pathway | 3.02456 | 0.048579 | 101.695 | 60 |
| Long-term depression | 3.02456 | 0.048579 | 101.695 | 60 |
| Natural killer cell mediated cytotoxicity | 2.96372 | 0.051627 | 98.9362 | 93 |

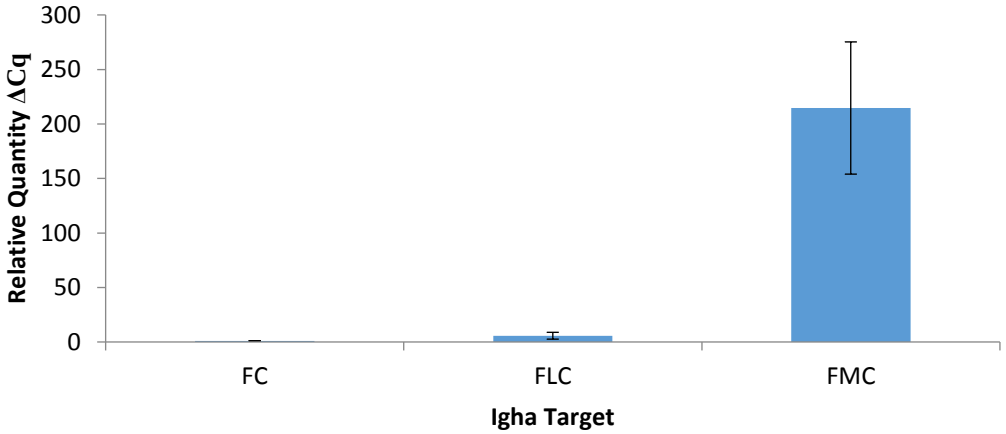


**Figure 17.** Igha gene expression determined via quantitative real-time PCR. Igha was significantly expressed in the FLC (low concentration - 40ppm) and FMC (medium concentration - 60ppm) animals relative to the control (FC - 0ppm) group.

# Chapter 4 Summary and Conclusion

## *4.1 Kidney Effects*

In summary, the short term effects of TDNF ingestion in Sprague Dawley rats was performed. Titanium fibers ranged from 50 nm to 950 nm in diameter. TDNF consumption seems to lead to a slight trend towards reduction in dietary ingestion. A literature search, however, indicates a lack of other studies showing any such effects. TDNF exposure showed no significant histopathological changes in renal tissues. However, LDH activity and Ti-47 concentration were found to be significantly elevated in the 40 ppm and 60 ppm rats. It has been previously shown that high levels of Ti-47 caused serious inflammation or even small cell lesions, which could correspond to the increased levels of LDH. This was followed with analysis of specific mRNA transcripts that might provide insight into the molecular perturbations with respect to TDNF ingestion. Up-regulation of $NF_KB$ likely indicates the involvement of renal tissue inflammation via an independent mechanism. Similarly, Gadd45a was significantly over expressed in kidney tissues. This transcript was previously increased following stressful growth arrest conditions and treatment with DNA-damaging agents.

## *4.2 Liver Effects*

The results indicate that TDNF (40 ppm and 60 ppm) is not toxic to the liver of Sprague Dawley rats during a short-term exposure via oral gavage. No significant changes in histopathological data, weight measurements, and serum ALB levels between 0 ppm and experimental groups are suggestive of little toxicity. In order to confirm this hypothesis, the hepatic effects of anatase-TDNF would need to be investigated in the future in addition to prolonged exposure periods and higher concentrations of TDNF.

*4.3 Lung Effects*

The present study was undertaken to examine the short-term toxicity associated with TDNF ingestion. Lung weight and qualitative examination of the lung showed no significant changes. However serum total protein and weight gain during the course of the study displayed marginal concentration-dependent alterations. These findings were followed by global gene expression analysis to identify which transcripts might be responsive to TDNF toxicity. Differentially expressed mRNA levels were dose-dependently higher in animals exposed to TDNF. It appears that the majority of the affected genes may be biochemically involved in immune response and inflammation. We surmise that TDNF may be too long to penetrate the cell, which may create a phagocytosis site and trigger inflammatory and immune response. All results taken together show that short-term ingestion of TDNF may produce moderate effects indicative of inflammation. Finally, the Igha gene was dose-dependently upregulated in treated groups in a manner similar to patterns noted in the genome-wide results.

## References

1. (a) Aslani, F.; Bagheri, S.; Julkapli, N. M.; Juraimi, A. S.; Hashemi, F. S. G.; Baghdadi, A., Effects of Engineered Nanomaterials on Plants Growth: An Overview. *Sci World J* **2014**; (b) Servin, A.; Elmer, W.; Mukherjee, A.; De la Torre-Roche, R.; Hamdi, H.; White, J. C.; Bindraban, P.; Dimkpa, C., A review of the use of engineered nanomaterials to suppress plant disease and enhance crop yield. *J Nanopart Res* **2015,** *17* (2).

2. (a) Holzinger, M.; Le Goff, A.; Cosnier, S., Nanomaterials for biosensing applications: a review. *Frontiers in chemistry* **2014,** *2*, 63; (b) Liu, X. D.; Zhong, Z. G.; Tang, Y. F.; Liang, B. Y., Review on the Synthesis and Applications of Fe3O4 Nanomaterials. *J Nanomater* **2013**.

3. (a) Chen, X.; Mao, S. S., Titanium dioxide nanomaterials: Synthesis, properties, modifications, and applications. *Chem Rev* **2007,** *107* (7), 2891-2959; (b) Suttiponparnit, K.; Jiang, J.; Sahu, M.; Suvachittanont, S.; Charinpanitkul, T.; Biswas, P., Role of Surface Area, Primary Particle Size, and Crystal Phase on Titanium Dioxide Nanoparticle Dispersion Properties. *Nanoscale research letters* **2011,** *6* (1), 27.

4. (a) Buzea, C.; Pacheco, I. I.; Robbie, K., Nanomaterials and nanoparticles: Sources and toxicity. *Biointerphases* **2007,** *2* (4), Mr17-Mr71; (b) Shi, H.; Magaye, R.; Castranova, V.; Zhao, J., Titanium dioxide nanoparticles: a review of current toxicological data. *Particle and fibre toxicology* **2013,** *10*, 15; (c) Weir, A.; Westerhoff, P.; Fabricius, L.; Hristovski, K.; von Goetz, N., Titanium dioxide nanoparticles in food and personal care products. *Environmental science & technology* **2012,** *46* (4), 2242-50.

5. Trouiller, B.; Reliene, R.; Westbrook, A.; Solaimani, P.; Schiestl, R. H., Titanium dioxide nanoparticles induce DNA damage and genetic instability in vivo in mice. *Cancer research* **2009,** *69* (22), 8784-9.

6. Park, E. J.; Yi, J.; Chung, K. H.; Ryu, D. Y.; Choi, J.; Park, K., Oxidative stress and apoptosis induced by titanium dioxide nanoparticles in cultured BEAS-2B cells. *Toxicology letters* **2008,** *180* (3), 222-9.

7. Coccini, T.; Grandi, S.; Lonati, D.; Locatelli, C.; De Simone, U., Comparative cellular toxicity of titanium dioxide nanoparticles on human astrocyte and neuronal cells after acute and prolonged exposure. *Neurotoxicology* **2015,** *48*, 77-89.

8. Brown, D. M.; Kinloch, I. A.; Bangert, U.; Windle, A. H.; Walter, D. M.; Walker, G. S.; Scotchford, C. A.; Donaldson, K.; Stone, V., An in vitro study of the potential of carbon

nanotubes and nanofibres to induce inflammatory mediators and frustrated phagocytosis. *Carbon* **2007,** *45* (9), 1743-1756.

9. (a) Colvin, V. L., The potential environmental impact of engineered nanomaterials (vol 21, pg 1166, 2003). *Nature biotechnology* **2004,** *22* (6), 760-760; (b) Iavicoli, I.; Leso, V.; Bergamaschi, A., Toxicological Effects of Titanium Dioxide Nanoparticles: A Review of In Vivo Studies. *J Nanomater* **2012**.

10. Ramkumar, K. M.; Manjula, C.; Gnanakumar, G.; Kanjwal, M. A.; Sekar, T. V.; Paulmurugan, R.; Rajaguru, P., Oxidative stress-mediated cytotoxicity and apoptosis induction by TiO2 nanofibers in HeLa cells. *European journal of pharmaceutics and biopharmaceutics : official journal of Arbeitsgemeinschaft fur Pharmazeutische Verfahrenstechnik e.V* **2012,** *81* (2), 324-33.

11. Wilcox, C. S., Reactive oxygen species: roles in blood pressure and kidney function. *Current hypertension reports* **2002,** *4* (2), 160-6.

12. (a) Choi, H. S.; Ashitate, Y.; Lee, J. H.; Kim, S. H.; Matsui, A.; Insin, N.; Bawendi, M. G.; Semmler-Behnke, M.; Frangioni, J. V.; Tsuda, A., Rapid translocation of nanoparticles from the lung airspaces to the body. *Nature biotechnology* **2010,** *28* (12), 1300-3; (b) Tang, J.; Xiong, L.; Wang, S.; Wang, J.; Liu, L.; Li, J.; Yuan, F.; Xi, T., Distribution, translocation and accumulation of silver nanoparticles in rats. *Journal of nanoscience and nanotechnology* **2009,** *9* (8), 4924-32.

13. Fontana, L.; Leso, V.; Marinaccio, A.; Cenacchi, G.; Papa, V.; Leopold, K.; Schindl, R.; Bocca, B.; Alimonti, A.; Iavicoli, I., The effects of palladium nanoparticles on the renal function of female Wistar rats. *Nanotoxicology* **2015,** *9* (7), 843-51.

14. Allegri, M.; Bianchi, M. G.; Chiu, M.; Varet, J.; Costa, A. L.; Ortelli, S.; Blosi, M.; Bussolati, O.; Poland, C. A.; Bergamaschi, E., Shape-Related Toxicity of Titanium Dioxide Nanofibres. *Plos One* **2016,** *11* (3).

15. (a) Gato, W. E.; Hales, D. B.; Means, J. C., Hepatic gene expression analysis of 2-aminoanthracene exposed Fisher-344 rats reveal patterns indicative of liver carcinoma and type 2 diabetes. *J Toxicol Sci* **2012,** *37* (5), 1001-1016; (b) Meggs, W. J.; Brewer, K. L., Weight gain associated with chronic exposure to chlorpyrifos in rats. *Journal of medical toxicology : official journal of the American College of Medical Toxicology* **2007,** *3* (3), 89-93.

16. Scown, T. M.; van Aerle, R.; Johnston, B. D.; Cumberland, S.; Lead, J. R.; Owen, R.; Tyler, C. R., High doses of intravenously administered titanium dioxide nanoparticles accumulate in the kidneys of rainbow trout but with no observable impairment of renal function. *Toxicological sciences : an official journal of the Society of Toxicology* **2009,** *109* (2), 372-80.

17. Gikins, M. C., C., Clinical Laboratory Parameters for Crl: WI (Han).

18. Alberghina, D.; Giannetto, C.; Vazzana, I.; Ferrantelli, V.; Piccione, G., Reference intervals for total protein concentration, serum protein fractions, and albumin/globulin ratios in clinically healthy dairy cows. *Journal of veterinary diagnostic investigation : official publication of the American Association of Veterinary Laboratory Diagnosticians, Inc* **2011,** *23* (1), 111-4.

19. McGreal, E. P.; Miller, J. L.; Gordon, S., Ligand recognition by antigen-presenting cell C-type lectin receptors. *Curr Opin Immunol* **2005,** *17* (1), 18-24.

20. Hur, E. M.; Patel, S. N.; Shimizu, S.; Rao, D. S.; Gnanapragasam, P. N.; An, D. S.; Yang, L.; Baltimore, D., Inhibitory effect of HIV-specific neutralizing IgA on mucosal transmission of HIV in humanized mice. *Blood* **2012,** *120* (23), 4571-82.

21. Loven, J.; Orlando, D. A.; Sigova, A. A.; Lin, C. Y.; Rahl, P. B.; Burge, C. B.; Levens, D. L.; Lee, T. I.; Young, R. A., Revisiting global gene expression analysis. *Cell* **2012,** *151* (3), 476-82.

22. Rogers, K. A.; Jayashankar, L.; Scinicariello, F.; Attanasio, R., Nonhuman primate IgA: genetic heterogeneity and interactions with CD89. *Journal of immunology* **2008,** *180* (7), 4816-24.

23. Sakai, E.; Bottaro, A.; Davidson, L.; Sleckman, B. P.; Alt, F. W., Recombination and transcription of the endogenous Ig heavy chain locus is effected by the Ig heavy chain intronic enhancer core region in the absence of the matrix attachment regions. *Proceedings of the National Academy of Sciences of the United States of America* **1999,** *96* (4), 1526-31.

24. Ovando, B. J.; Vezina, C. M.; McGarrigle, B. P.; Olson, J. R., Hepatic gene downregulation following acute and subchronic exposure to 2,3,7,8-tetrachlorodibenzo-p-dioxin. *Toxicological sciences : an official journal of the Society of Toxicology* **2006,** *94* (2), 428-38.

25. Wisnewski, A. V.; Liu, J.; Colangelo, C. M., Glutathione reaction products with a chemical allergen, methylene-diphenyl diisocyanate, stimulate alternative macrophage activation and eosinophilic airway inflammation. *Chemical research in toxicology* **2015,** *28* (4), 729-37.